研究成果の刊行に関する一覧表

雑誌

発表者氏名	論文タイトル名	発表誌名，巻号：ページ，出版年
Uezumi A, Ojima K, Fukada S, Ikemoto M, Masuda S, Miyagoe- Suzuki Y, Takeda S:	Functional heterogeneity of side population cells in skeletal muscle.	***Biochem Biophys Res Commun***, 341: 864-73, 2006
Ampong BN, Imamura M, Matsumiya T, Yoshida M, Takeda S:	Instracellulat localization of Dysferlin and its association with the Dihydropyridine receptor.	***Acta Myologica***, XXIV: 134-144, 2005
Shimatsu Y, Yoshimura M, Yuasa K, Urasawa N, Tomohiro M, Nakura M, Tanigawa M, Nakamura A, Takeda S:	Major clinical and histopathological characteristics of canine X-linked muscular dystrophy in Japan, CXMD$_J$.	***Acta Myologica***, XXIV: 145-154, 2005
Mochizuki Y, Ojima K, Uezumi A, Masuda S, Yoshimura K, Takeda S.	Participation of bone marrow-derived cells in fibrotic changes in denervated skeletal muscle.	***Am J Pathol***, 166(6): 1721-32, 2005
Ishiura S., Kino Y, Nezu Y, Onishi H, Ohno E, Sasagawa N:	Regulation of splicing by MBNL and CELF family of RNA- binding protein.	***Acta Myologica***, XXIV: 74-77, 2005
Oma Y, Kino Y, Sasagawa N, S. Ishiura:	Comparative analysis of the cytotoxicity of homopolymeric amino acids.	***Biochimica et Biophysica Acta,*** 1748: 174-179, 2005
H. Mitsuhashi, A. Yoshikawa, N. Sasagawa, Y. Hayashi, S. Ishiura:	Denervation Enhances the Expression of SHPS-1 in Rat Skeletal Muscle.	***J Biochem,*** 137(4): 495-502, 2005

Available online at www.sciencedirect.com
SCIENCE DIRECT
ELSEVIER
Biochemical and Biophysical Research Communications 341 (2006) 864–873
BBRC
www.elsevier.com/locate/ybbrc

Functional heterogeneity of side population cells in skeletal muscle

Akiyoshi Uezumi, Koichi Ojima, So-ichiro Fukada, Madoka Ikemoto, Satoru Masuda, Yuko Miyagoe-Suzuki, Shin'ichi Takeda *

Department of Molecular Therapy, National Institute of Neuroscience, National Center of Neurology and Psychiatry, 4-1-1 Ogawa-higashi, Kodaira, Tokyo 187-8502, Japan

Received 18 December 2005
Available online 23 January 2006

Abstract

Skeletal muscle regeneration has been exclusively attributed to myogenic precursors, satellite cells. A stem cell-rich fraction referred to as side population (SP) cells also resides in skeletal muscle, but its roles in muscle regeneration remain unclear. We found that muscle SP cells could be subdivided into three sub-fractions using CD31 and CD45 markers. The majority of SP cells in normal non-regenerating muscle expressed CD31 and had endothelial characteristics. However, $CD31^-CD45^-$ SP cells, which are a minor subpopulation in normal muscle, actively proliferated upon muscle injury and expressed not only several regulatory genes for muscle regeneration but also some mesenchymal lineage markers. $CD31^-CD45^-$ SP cells showed the greatest myogenic potential among three SP sub-fractions, but indeed revealed mesenchymal potentials in vitro. These SP cells preferentially differentiated into myofibers after intramuscular transplantation in vivo. Our results revealed the heterogeneity of muscle SP cells and suggest that $CD31^-CD45^-$ SP cells participate in muscle regeneration.

Keywords: Side population cells; Muscle regeneration; Mesenchymal differentiation; Transplantation

Adult skeletal muscles have a remarkable ability to regenerate following muscle damage. This regeneration has been attributed to satellite cells that reside between the sarcolemma and the basal lamina. Satellite cells are quiescent mononucleated cells in normal conditions, however, in response to muscle damage, they become activated, proliferate, and then exit the cell cycle either to renew the quiescent satellite cell pool or to differentiate into mature myofibers. Thus, they have been considered to be the myogenic precursor cells that give rise to myoblasts and the sole source of adult myogenic cells [1].

In 1998, Ferrari et al. [2] have demonstrated for the first time that bone marrow (BM)-derived cells contribute to the skeletal muscle after BM transplantation. Side population (SP) cells were first identified in bone marrow based on the ability to exclude Hoechst 33342 dye as an enriched fraction of hematopoietic stem cells (HSCs) [3]. later, it has been reported that they also participate in muscle regeneration [4]. Studies using whole BM cells showed that BM-derived mononucleated cells display several characteristics of satellite cells, suggesting that donor-derived BM cells contribute to muscle fibers in a stepwise biological progression [5,6]. However, using single HSC transplantation experiment, Camargo et al. [7] suggested that cells committed to the myeloid lineage contribute to muscle through fusion event. Therefore, multiple mechanisms underlay contribution of BM-derived cells to skeletal muscle regeneration.

SP cells have been also identified in skeletal muscle [4]. Muscle SP cells cannot only reconstitute the hematopoietic system of lethally irradiated mice [4,8], but also differentiate into skeletal muscle cells [4,9]. Furthermore, they have been reported to participate in vascular regeneration [10]. Several lines of evidence suggest that muscle SP cells are a cell population distinct from satellite cells [9,11–13]. While muscle SP cells possess these attractive

* Corresponding author. Fax: +81 42 346 1750.
E-mail address: takeda@ncnp.go.jp (S. Takeda).

0006-291X/$ - see front matter © 2006 Elsevier Inc. All rights reserved.
doi:10.1016/j.bbrc.2006.01.037

features, they have been reported to be heterogeneous population. In fact, muscle SP cells contain both $CD45^+$ and $CD45^-$ cells, and hematopoietic potential has been exclusively found in $CD45^+$ fraction [8,9]. As regards the myogenic potential, both $CD45^+$ and $CD45^-$ fractions have been shown to differentiate into skeletal muscle cells [9,14], but there is no comparative study dealing with subpopulation of muscle SP cells during muscle regeneration.

In the present study, we have further divided muscle SP cells into three sub-fractions using CD31 and CD45, examined the properties of each sub-fraction, and identified a novel subpopulation ($CD31^-CD45^-$ SP cells) that showed the greatest myogenic potential both in vitro and in vivo. These results provide a new insight for stem cell-based therapy of muscular dystrophy.

Materials and methods

Animals. All procedures using experimental animals were approved by the Experimental Animal Care and Use Committee at the National Institute of Neuroscience. Eight- to ten-week-old C57BL/6 mice were purchased from Nihon CLEA (Japan). GFP Tg mice were provided by Dr. M. Okabe (Osaka University) and used in cell transplantation experiments. NOD/*scid* mice provided by the Institute for Experimental Animals, Japan, were used as recipients.

To induce muscle regeneration, 100 μl of CTX (10 μM in saline, Wako Chemicals) was injected into the tibialis anterior (TA) muscle with a 29-gauge needle. In FACS analysis experiments, CTX was injected into TA (50 μl), gastrocnemius (50 μl), and quadriceps femoris muscles (25 μl).

BM transplantation was performed as previously described [14]. Mice were subjected to analysis 12 weeks after transplantation.

Antibodies. Mouse Bcrp-1 cDNA was provided by Dr. A.H. Schinkel [15]. A DNA fragment corresponding to cytoplasmic domain of Bcrp1, amino acids 300–337, was fused to GST in a pGEX-4T-2 vector (Amersham Biosciences), and the fusion protein was used to immunize rabbits. The serum obtained was affinity-purified. Other antibodies used in these studies are listed in Table S1.

Cell preparation and FACS analysis. Muscle-derived mononucleated cells were prepared from C57BL/6 mice, GFP Tg mice, or GFP-BM transplanted mice as previously described [14]. Hoechst staining was performed as described by Goodell et al. (http//www.bcm.tmc.edu/genetherapy/goodell/new_site/protocols.html). Cells were re-suspended at 10^6 cells per ml in DMEM (Invitrogen) containing 2% FBS (Trace Biosciences), 10 mM Hepes, and 5 μg/ml Hoechst 33342 (Sigma), and incubated for 90 min at 37 °C in the presence or the absence of 50 μM verapamil (Sigma). During incubation, cells were mixed 3–4 times. For analysis of Ac-LDL uptake, 10 μg/ml DiI-labeled Ac-LDL (Biomedical Technologies) was added. After antibody staining, cells were re-suspended in PBS containing 2.5% FBS and 2 μg/ml propidium iodide (PI) (BD PharMingen). Cell sorting was performed on a FACS VantageSE flow cytometer (BD Biosciences). Debris and dead cells were excluded by forward scatter, side scatter, and PI gating. Cell viability after staining and sorting was comparable to that previously reported [14].

RNA extraction and RT-PCR. Total RNA was extracted from 1×10^4 FACS sorted cells by using a RNeasy Micro Kit (Qiagen) and then reverse transcribed into cDNA by using TaqMan Reverse Transcription Reagents (Roche). The PCRs were performed with 1 μl cDNA product under the following cycling conditions: 94 °C for 3 min followed by 40 cycles of amplification (94 °C for 15 s, 60 °C for 30 s, and 72 °C for 30 s) with a final incubation at 72 °C for 5 min. Specific primer sequences used for PCR are available on request.

Cell culture. SP cells were cultured alone with growth medium (GM); DMEM containing 20% FBS and 2.5 ng/ml bFGF (Invitrogen) in chamber slides (Nalge Nunc) coated with Matrigel (BD Biosciences) for 3–5 days. For osteogenic differentiation, the medium was changed to a differentiation medium (DM), 5% horse serum in DMEM supplemented with or without 500 ng/ml recombinant human BMP2 (R&D Systems), and cultured for 4–6 days. For adipogenic differentiation, cells were exposed to 3 cycles of 3 days of adipogenic induction medium (Cambrex Bioscience) followed by 1 day of adipogenic maintenance medium (Cambrex Bioscience) and then cells were maintained for five more days in the adipogenic maintenance medium. Alkaline phosphatase (AP) was stained using Sigma kit #85 according to the manufacturer's instructions. To stain lipids, cells were fixed in 10% formalin, rinsed in water and then 60% isopropanol, stained with Oil red O in 60% isopropanol, and rinsed in water. For myogenic differentiation, muSP-31, muSP-45, or muSP-DN purified from GFP Tg mice were co-cultured with myoblasts prepared from C57BL/6 mice as previously described [16,17] in GM. DM was supplied 3–5 days after starting co-culture.

Osteogenic activity and myotube-forming activity were determined by the following formulas: osteogenic activity = [the number of AP^+ cells in seven randomly selected fields (corresponding to one-tenth of the whole area of the well)]/(the number of seeded cells) and myotube-forming activity = (the number of GFP^+ myotubes in seven randomly selected fields)/(the number of seeded cells). In order to measure the extent of adipogenic differentiation, stained oil droplets were extracted for 5 min with 100 μl of 4% Nonidet P-40 in isopropanol, and the absorbance of the dye-triglyceride complex was measured at 520 nm [18]; then, adipogenic activity was determined by the following formula: (the absorbance at 520 nm)/(the number of seeded cells).

Intramuscular transplantation experiments. muSP-DN or muSP-31 cells were purified from GFP Tg mice and were injected directly into the TA muscles of NOD/*scid* mice. One day before transplantation, host TA muscles were treated with CTX. The number of transplanted cells is indicated in Table 1. Three weeks after transplantation, TA muscles were excised and fixed in 4% PFA for 30 min, immersed sequentially in 10% sucrose/PBS and 20% sucrose/PBS, and frozen in isopentane cooled with liquid nitrogen.

Immunohistochemistry. FACS sorted cells were collected by Cytospin3 (ThermoShandon). Cells were fixed with 4% PFA for 5 min. Frozen muscle tissues were sectioned using a cryostat. Specimens were blocked with 5% goat serum (Cedarlane) in PBS for 15 min and incubated with primary antibodies at 4 °C overnight, followed by secondary staining. Stained cells were mounted in Vectashield with DAPI (Vector) and photographed using a fluorescence microscope IX70 (OLYMPUS) equipped with a QuantixTM air-cooled CCD camera (Photometrics) and IP Lab software (Scanalytics Inc.). Stained muscle sections were counterstained with TOTO-3 (1:5000; Molecular Probes), then mounted in Vectashield (Vector), and observed under the confocal laser scanning microscope system TCSSP (Leica).

Statistics. Values were expressed as means ± SD or ± SEM. Statistical significance was assessed by Student's *t* test. In comparison of more than two groups, one-way analysis of variance (ANOVA) followed by the Fisher's PLSD was used. A probability of less than 5% ($P < 0.05$) or 1% ($P < 0.01$) was considered statistically significant.

Table 1
Appearance of GFP^+ myofibers after intramuscular transplantation

Cell type	Experiment No.	Number of injected cells/TA muscle	Number of GFP^+ myofibers/TA muscle
muSP-DN cells	Ex. 1	1.7×10^3	14
	Ex. 2	2.5×10^3	9
	Ex. 3	2.5×10^3	0
muSP-31 cells	Ex. 1	1.6×10^4	3
	Ex. 2	1.6×10^4	0
	Ex. 3	1.6×10^4	0

Results

Most muscle SP cells are found in a subset of capillary or vein endothelial cells in non-regenerating skeletal muscle

We identified verapamil-sensitive SP cells in skeletal muscle after Hoechst staining (Fig. 1A) and analyzed the expression of several markers on them. The majority of muscle SP cells were $CD31^+$, usually recognized as a marker of endothelial cells (Figs. 1B–E), and negative for a pan-hematopoietic marker, CD45 (Fig. 1B). More than half of muscle SP cells were $CD34^+$, and $Sca\text{-}1^+$ cells comprised 90% of muscle SP cells (Figs. 1C and D). Compared to FACS profiles of whole-muscle-derived cells, SP cells were enriched in $Sca\text{-}1^+$ cells (Fig. S1). More than 85% of muscle SP cells were $CD31^+$ and took up acetylated low-density lipoprotein (Ac-LDL), a functional marker for endothelial cells and macrophages (Fig. 1E). These results indicate that most muscle SP cells have endothelial characteristics. Only cells in the main population (MP) were found to be $Pax7^+$, indicating that SP cells do not include muscle satellite cells (data not shown).

To examine the localization of muscle SP cells, we generated a rabbit polyclonal anti-mouse Bcrp1 antibody, because it has been reported that Bcrp1 is the major determinant of the SP phenotype [19]. Our antibody clearly recognized Bcrp1 expression in liver, small intestine, and kidney, as previously reported (Fig. S2) [20,21]. We confirmed that Bcrp1 antibody recognizes more than 80% of SP cells and less than 3% of MP cells collected by cytospin (Figs. 1F and G). In skeletal muscle, $Bcrp1^+$ cells were found outside the muscle basal lamina (Fig. 1H), which clearly distinguished $Bcrp1^+$ cells from satellite cells. Next, Bcrp1 expression in the vascular system was investigated. CD31 staining identified all endothelia from larger vessels to capillaries in muscle sections. Intriguingly, Bcrp1 was expressed by CD31-expressing endothelial cells, and its expression was preferentially observed on a subpopulation of capillary endothelium (Figs. 1I–K) and venous endothelium surrounded by thin vessel walls, as revealed by α-smooth muscle actin (αSMA) expression (Figs. 1L–N). These results, together with the results of FACS analysis, strongly suggest that the majority of muscle SP cells are a subset of endothelial cells present in capillaries or veins in non-regenerating skeletal muscle.

Behavior of muscle SP cells during muscle regeneration

We next examined the kinetics of SP cells during muscle regeneration induced by injection of cardiotoxin (CTX). After CTX injection, the total number of mononuclear cells per muscle weight gradually increased, with a peak at day 3. The number of SP cells also increased and reached its peak at day 3 (Fig. 2A). Muscle SP cells could be divided into three subpopulations based on CD31 and CD45 expression: $CD31^+CD45^-$ SP cells (designated muSP-31 cells), $CD31^-CD45^+$ SP cells (muSP-45 cells), and $CD31^-CD45^-$ SP cells (muSP-DN cells). muSP-31 cells and muSP-DN cells distributed throughout the SP tail, but muSP-45 cells were located close to the shoulder (data not shown). The majority of muscle SP cells in untreated muscle were muSP-31 cells (Fig. 1B). During regeneration, however, muSP-45 cells and muSP-DN cells increased in both their ratios and their numbers (Figs. 2B and C). Although $CD45^+$ cells were abundant in whole muscle-derived cells during regeneration and most of them were F4/80 antigen-positive mature macrophages, SP cells did not contain any mature inflammatory cells, as previously reported (data not shown) [14].

To clarify the origin of each subpopulation of SP cells, BM transplantation experiments were performed. We confirmed that muSP-45 cells were mobilized from bone marrow as previously reported (Figs. 3A and B) [14]. In contrast, both $CD45^-$ SP fractions are residents of skeletal muscle (Figs. 3A and B), consistent with the results reported by Rivier et al. [22].

Next, to determine whether each subpopulation of SP cells proliferates in damaged muscle, cells were stained with Ki67 antibody. Most muSP-45 cells (Figs. 3C and D) and muSP-31 cells (Figs. 3G and H) prepared from regenerating muscle were negative for Ki67, suggesting that the proliferation activities of these two fractions were low. On the other hand, about 60% of muSP-DN cells were positive for Ki67 (Figs. 3E and F), indicating that muSP-DN cells actively proliferated during muscle regeneration.

We next examined Bcrp1 expression on three sub-fractionated SP cells and found that only muSP-31 cells were Bcrp1-positive (Fig. 3K). These results suggest that some ABC transporters other than Bcrp1 are responsible for the phenotype of $CD31^-$ SP cells.

Gene expression of muscle SP cells during muscle regeneration

Our analysis revealed that each subpopulation of SP cells showed distinct kinetics during muscle regeneration. To better understand the traits of muscle SP cells, we analyzed gene expression during muscle regeneration. Three subpopulations of SP cells (in following experiments, muSP-45 cells from untreated muscle were omitted because of their low yield) or MP cells were collected from each time point during muscle regeneration, and RT-PCR was performed. We chose several myogenic (*Pax3*, *Pax7*, and *myf5*), endothelial (*Tie2*, *Flk1*, and *vWF*), and mesodermal-mesenchymal-associated (*αSMA*, *PPARγ*, *Runx2*, *PDGFRα*, and *PDGFRβ*) genes to clarify lineage characteristics of the target cells. We also examined expression of genes of developmental regulators (*msx1*, *Frizzled4* (*Fzd4*), *Patched1* (*Ptc1*), and *BMPR1A*), angiogenic factors (*angiopoietin-1* (*ang1*) and *VEGF*), and TGF-β superfamily antagonists (*follistatin* and *DAN*). muSP-DN cells from untreated muscles expressed only *PDGFRβ*, *Ptc1*, *ang1*, *follistatin*, and *DAN* (Fig. 4, cont. lane 1). Neither myogenic nor other lineage-specific markers could be detected in

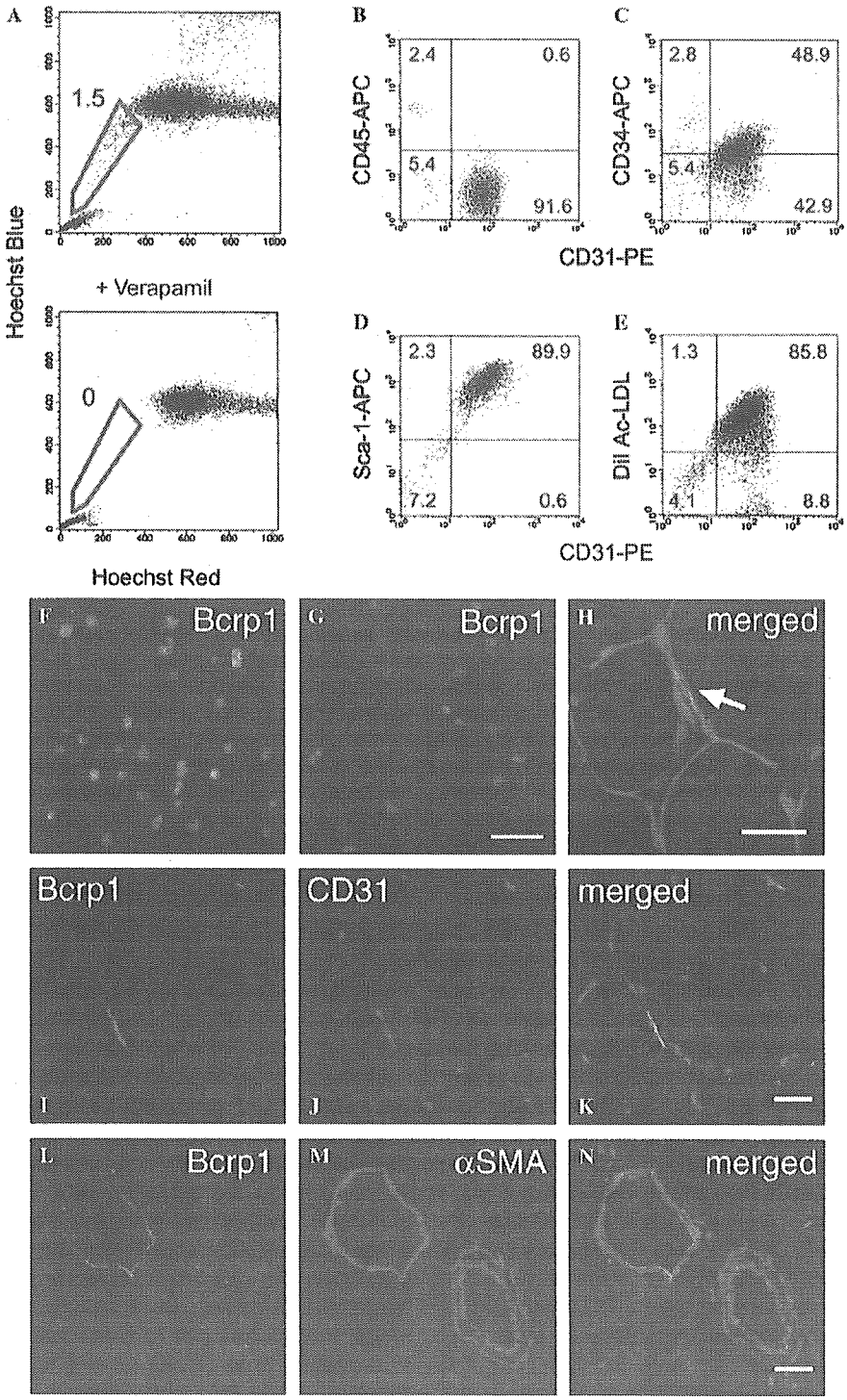

Fig. 1. Characterization of skeletal muscle SP cells. (A) Flow cytometric analysis of muscle-derived mononucleated cells after Hoechst 33342 staining with (lower panel) or without Verapamil (upper panel). The numbers indicate the percentage of SP cells (blue pentagons) in all mononucleated cells. (B–E) The expression of CD45 (B), CD34 (C), Sca-1 (D), and DiI-Ac-LDL uptake (E), and CD31 (B–E) on muscle SP cells. The percentage of cells in each quadrant is shown in the panel. (F,G) Immunofluorescent staining for Bcrp1 (green) and DAPI counterstaining (blue) of freshly sorted SP (F) and MP (G) cells. Immunofluorescent staining for Bcrp1 (green) and laminin α2 chain (red) (H), Bcrp1 (green) and CD31 (red) (I–K), and Bcrp1 (green) and α-smooth muscle actin (red) (L–N). TOTO-3 nuclear staining is shown in merged images (blue in H, K, and N). Bcrp1-positive cells are located outside the basal lamina (arrow), and they are partially overlapped with endothelial cells of capillary (I–K) and vein (L–N). Bars: 50 μm in (F,G), 20 μm in (H–N).

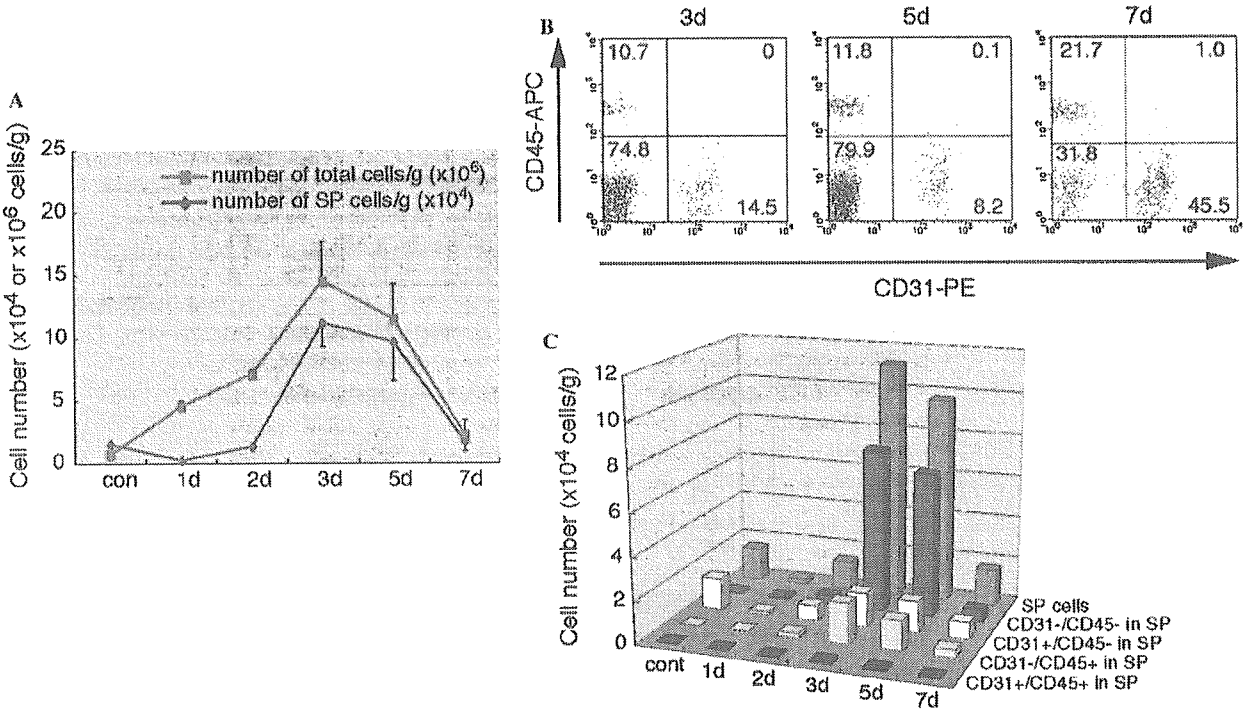

Fig. 2. Behavior of subpopulations of SP cells during muscle regeneration. (A) At 1 day (1d), 2 days (2d), 3 days (3d), 5 days (5d), and 7 days (7d) after CTX injection, the number of total cells (pink line) and SP cells (blue line) per gram of muscle weight was quantified. (B) At 3 days (3d), 5 days (5d), and 7 days (7d) after CTX injection, muscle SP cells prepared from regenerating muscle were analyzed for CD31 and CD45 expression. (C) Cell numbers in subpopulations of SP cells. muSP-45 cells (light blue bar) and muSP-DN cells (dark red bar) were significantly increased in number during muscle regeneration. Values (A,C) are the average of three independent experiments. Error bars represent SD.

this population indicating that muSP-DN cells do not contain cells committed to the lineages tested. At day 3 after CTX injection, muSP-DN cells began to express developmental regulator genes (Fig. 4, 3d, lane 1), and then at day 5, they also began to express several other lineage-specific genes (*Tie2*, *αSMA*, *PPARγ*, and *Runx2*). Angiogenic factors and TGF-β superfamily antagonists were also strongly expressed at this time point (Fig. 4, 5d, lane 1). In contrast, muSP-31 cells continuously expressed all three endothelial genes analyzed throughout the regeneration process (Fig. 4, lane 2). Expression of mature endothelial marker, such as *vWF*, suggests that muSP-31 cells represent committed endothelial cells. muSP-45 cells expressed only low levels of *αSMA*, *PDGFRβ*, and *follistatin* at day 5 after CTX injection (Fig. 4, lane 3). Myogenic markers, *Pax7* and *myf5*, were detected only in the MP fraction (Fig. 4, MP) indicating that myogenic cells are completely sorted into the MP fraction even during the process of muscle regeneration.

Differentiation potential of muscle SP cells for mesenchymal lineages

muSP-DN cells showed a unique gene expression pattern during muscle regeneration process: they began to express several mesenchymal genes at a late phase of muscle regeneration. Therefore, we examined the mesenchymal potentials of muscle SP subpopulations. muSP-DN cells from untreated muscle readily gave rise to alkaline phosphatase (AP)-positive cells when cultured in the presence of bone morphogenetic protein 2 (BMP2) (Figs. 5A and C). With adipogenic induction, they also differentiated into adipocytes containing numerous lipid droplets in the cytoplasm (Figs. 5A and D). Reflecting the results of gene expression analysis, muSP-DN cells from regenerating muscle more efficiently differentiated into osteogenic cells and adipocytes than those from untreated muscle did (Figs. 5B–D). Unexpectedly, muSP-DN cells from regenerating muscle also differentiated into adipocytes without adipogenic induction (Figs. 5B and D), suggesting that they are susceptible to adipogenesis under our culture condition. In contrast, muSP-31 cells did not possess these differentiation potentials (Figs. 5A–D). Nor did muSP-45 cells, which were dramatically mobilized from BM into regenerating muscle (Figs. 5B–D). The attribute of differentiation potential is therefore a feature of muSP-DN.

Myogenic potential of muscle SP cells in vitro

We next evaluated the myogenic potential of muscle SP cells in vitro. When SP cells were cultured alone, they never differentiated into skeletal muscle cells (data not shown). Each subpopulation of SP cells was prepared from GFP Tg mice and co-cultured with wild type (WT) primary

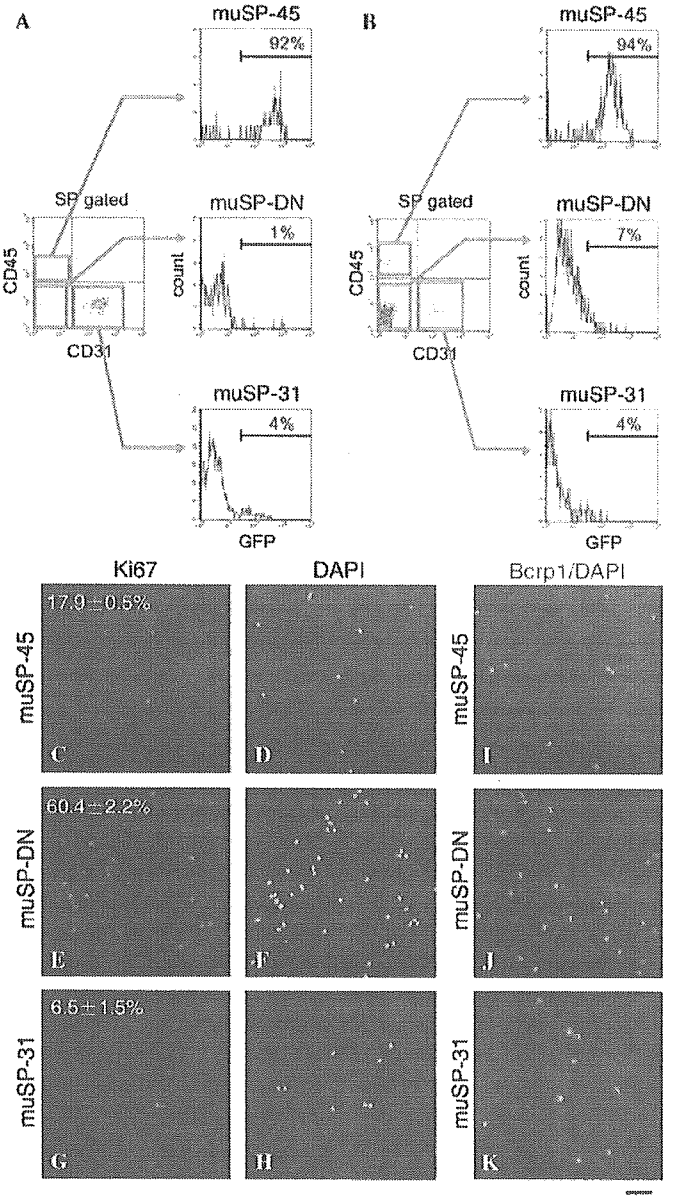

Fig. 3. Origin, proliferative activity, and Bcrp1 expression of subpopulations of muscle SP cells. (A,B) C57BL/6 mice were transplanted with whole BM from GFP Tg mice, and 3 months later, SP cells from untreated muscle (A) or regenerating muscle (3 days after CTX injection) (B) were further analyzed for CD31, CD45, and GFP expression. Note that CD45 SP cells (middle and lower panels) are almost all negative for GFP, indicating that they do not originate from BM. In contrast, more than 90% of muSP-45 cells were GFP^+ (upper panels). (C–H) Ki67 expression (green) and nuclei stained with DAPI (blue) on muSP-45 (C,D), muSP-DN (E,F), and muSP-31 (G,H) cells. The percentages of Ki67-positive cells were expressed as means ± SD of three independent experiments. muSP-45 (I), muSP-DN (J), and muSP-31 (K) were sorted from regenerating muscle and stained for Bcrp1 (green) and nuclei (blue). Only muSP-31 cells were stained positive for Bcrp1 (K). Bar: 50 μm.

myoblasts derived from satellite cells. muSP-DN cells from untreated muscle rapidly proliferated in vitro as observed in regenerating muscle (Fig. 2C). On the contrary, muSP-31 cells hardly expanded. After 2–3 weeks co-culture, both muSP-DN cells and muSP-31 cells differentiated not only into multinucleated myotubes co-expressing GFP and sarcomeric-α-actinin (Figs. 5E–G, only muSP-DN culture is shown) but also mononucleated myocytes (shown in insets). The frequency of mononucleated myocytes was too low to quantify, but existence of these cells suggests that myogenic differentiation of SP cells could occur without fusion. Strikingly, the myotube-forming activity (the frequency of GFP^+ myotubes, see Materials and methods for details) of muSP-DN cells was approximately 10-fold that of muSP-31 cells (Fig. 5H, lane for cont. $0.026 + 0.007$ vs $0.002 + 0.001$). In the experiments using SP cells from regenerating muscle at 3 days after CTX injection, muSP-DN cells showed the highest

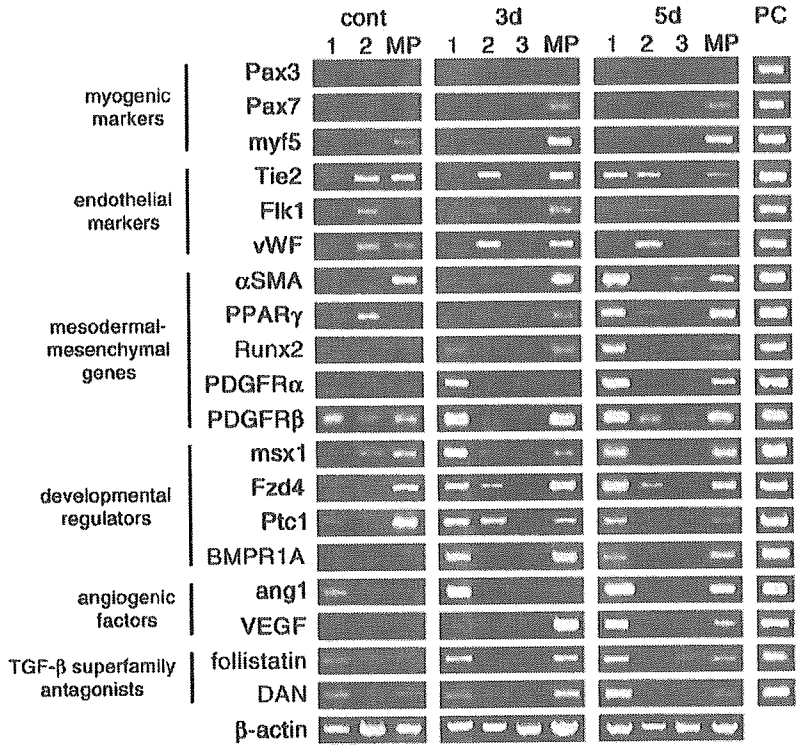

Fig. 4. Gene expression profiles of muscle SP cells during muscle regeneration. muSP-DN (lane 1), muSP-31 (lane 2), muSP-45 (lane 3), or MP cells were collected from untreated (cont) and regenerating muscle at 3 days (3d) or 5 days (5d) after CTX injection, and RT-PCR was performed against the indicated genes. Total embryo extract (E13) was used as a positive control (PC). β-actin was amplified to confirm that the quantities of mRNA were equal.

myotube-forming activity, although each SP subpopulation did form myotubes co-expressing GFP and sarcomeric-α-actinin (Fig. 5H, lane for CTX3d). This clearly demonstrates that muSP-DN cells have the highest myogenic potential among SP sub-fractions in vitro. For comparison, we quantified the myotube-forming activity of satellite cell-derived myoblasts. The value was 0.09 ± 0.01, indicating that myogenic activity of myoblasts is much higher than that of muSP-DN cells.

Myogenic potential of muscle SP cells in vivo

To evaluate the myogenic potential of muscle SP cells in vivo, we performed transplantation experiments. muSP-DN or muSP-31 cells from untreated muscle of GFP Tg mice were directly transplanted into CTX-treated TA muscles of immunodeficient NOD/*scid* mice. Three weeks after transplantation, muSP-DN cells had generated myofibers more efficiently than muSP-31 cells (Figs. 6A and B, and Table 1), indicating that muSP-DN cells had relatively higher myogenic potential in vivo as well as in vitro. Contrary to our expectation, muSP-DN cells formed no GFP-positive adipocytes after transplantation.

Discussion

Muscle SP cells have been suggested to be multipotent and can contribute to skeletal muscle regeneration [4,9,10,23]. However, most of these studies dealt with whole muscle SP cells as one functional unit. We subdivided, for the first time, muscle SP cells using CD31 and CD45 markers and revealed functional heterogeneity of muscle SP cells. $CD31^{+}CD45^{-}$ SP cells (muSP-31 cells) are a main subpopulation in non-regenerating muscle, but $CD31^{-}CD45^{-}$ SP cells (muSP-DN cells) which represent a minor subpopulation in non-regenerating muscle have the greatest differentiation potentials and become predominant subpopulation of SP cells upon muscle injury.

Differentiation potential of muscle SP cells

Phenotypic and immunohistochemical analysis suggested that muSP-31 cells are a subset of endothelial cells of capillaries and veins. They poorly proliferate after injury or in in vitro culture, and their differentiation potentials are limited both in vitro and in vivo.

$CD45^{+}$ muscle SP cells (muSP-45 cells) were shown to have both hematopoietic and myogenic potentials, and hematopoietic potential of muscle-derived cells was exclusively found in this fraction [8,9]. We previously reported the contribution of muSP-45 cells to muscle regeneration [14]. In this study, we identified novel subpopulation that possesses much higher myogenic potential than muSP-45, muSP-DN.

muSP-DN cells showed the highest differentiation potential of all the mesenchymal lineages tested among

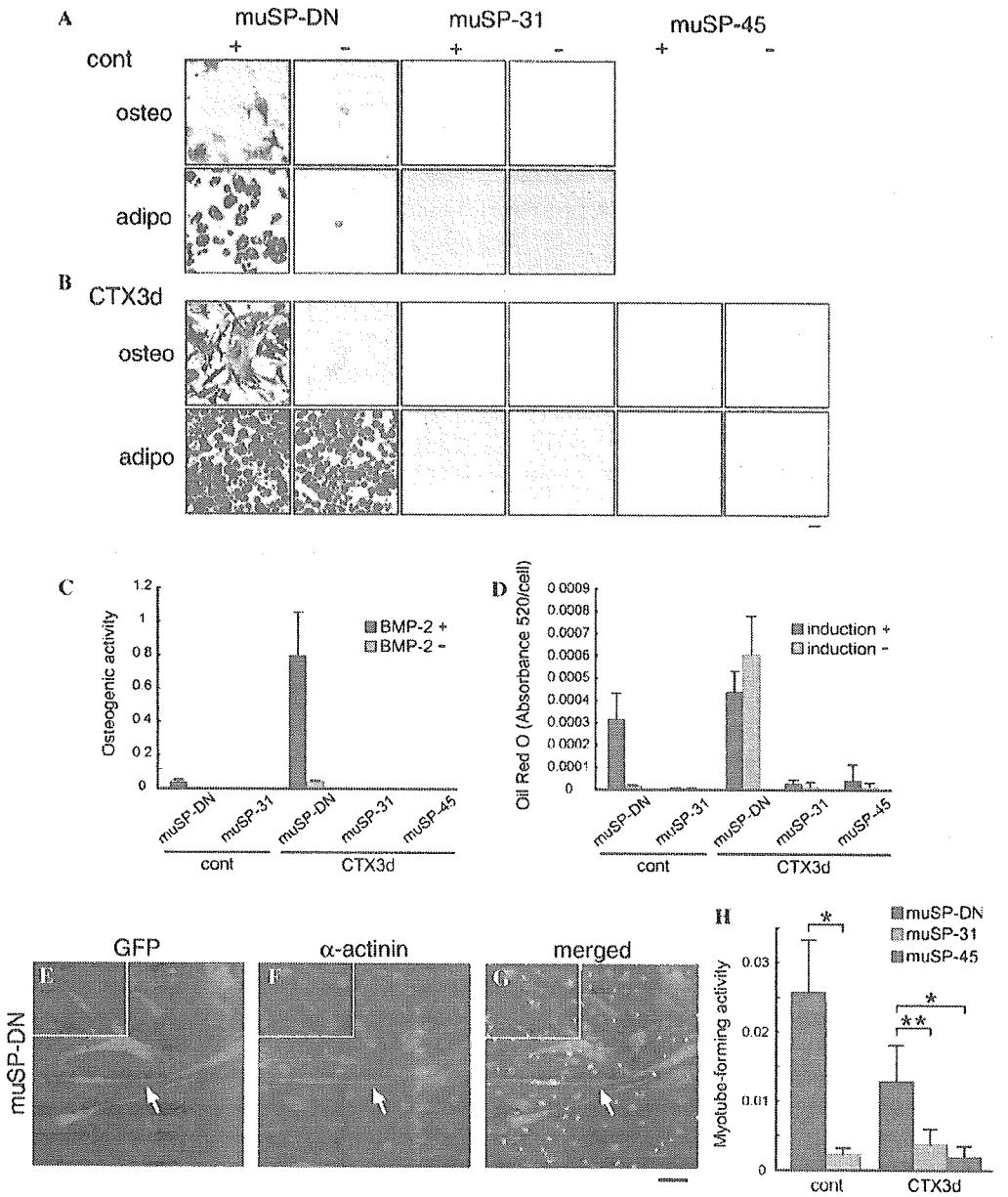

Fig. 5. muSP-DN cells differentiate into osteogenic cells, adipocytes, and skeletal muscle cells. (A,B) Three subpopulations of SP cells prepared from untreated (A) or regenerating (B) muscle were induced to differentiate into osteogenic or adipogenic cells. Uninduced cells (−) and induced cells (+) were then examined for alkaline phosphatase expression (osteo) or oil deposits (adipo). Bar: 50 μm. (C,D) Osteogenic (C) and adipogenic (D) activities of subsets of SP cells prepared from control (cont) or regenerating muscle at 3 days after CTX injection (CTX3d) were quantified. Values are the average of three independent experiments. Error bars represent SD. (E–G) Co-culture of muscle SP cells with myoblasts. muSP-DN cells from GFP Tg mice were sorted and co-cultured with WT primary myoblasts in differentiation medium. Cells were stained with anti-GFP (green) and anti-sarcomeric α-actinin (red) antibodies. Nuclear staining with DAPI (blue) is shown in merged images (G). Insets show GFP^+ mononucleated myocyte. Bar: 50 μm. (H) Myotube-forming activities of muSP-DN cells (red bars), muSP-31 cells (blue bars), and muSP-45 cells (green bar) are shown. Each subpopulation was prepared from untreated (cont) or CTX-treated regenerating muscle (CTX3d). Values are the average of three independent experiments. Error bars represent SD. $^*P < 0.01$, $^{**}P < 0.05$.

SP subpopulations. They were negative for lineage-specific markers under the non-regenerating condition, but after muscle injury or in in vitro expansion, they actively proliferated and were readily induced to express several mesenchymal genes. Their differentiation potential seems to be restricted to mesenchymal lineages because we did not detect hematopoietic colonies derived from muSP-DN cells in vitro and muSP-DN cells failed to rescue the lethally irradiated mice (data not shown). These observations indicate that muSP-DN cells are enriched for primitive mesenchymal cells. This notion is further supported by gene expression pattern of muSP-DN cells. muSP-DN cells

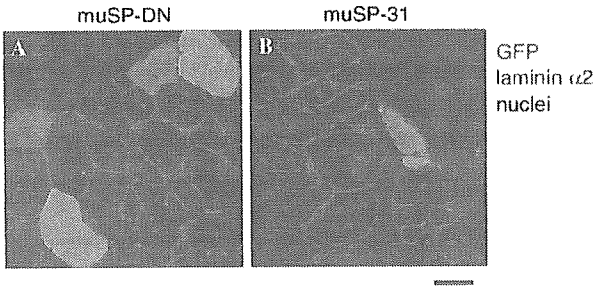

Fig. 6. muSP-DN cells participate in myofiber formation during muscle regeneration. (A,B) muSP-DN (A), muSP-31 (B) were transplanted into CTX-injected NOD/*scid* muscles. Each subpopulation was prepared from untreated muscle of GFP Tg mice. Muscle sections were stained with anti-GFP (green) and anti-laminin α2 (red) antibodies 3 weeks after transplantation. More GFP-positive myofibers were detected in muSP-DN-transplanted muscles (A) than in muscles transplanted with muSP-31 cells (B). Bar: 40 μm.

specifically expressed *ang1* under the non-regenerating condition and during the early phase of regeneration (Fig. 4, lane 1, cont or 3d). Perivascular cells, such as pericytes, express ang1 [24,25], and several groups suggest that multipotent mesenchymal stem cells may be derived from pericytes [26–28]. A recent report demonstrated that vascular mural precursor cells are negative for endothelial markers but positive for Tie2 and smooth muscle cell markers [29]. Likewise, muSP-DN cells were negative for *Flk1* and *vWF* throughout the regeneration process (Fig. 4, lane 1), but began to express *Tie2* and *αSMA* during late phases of regeneration (Fig. 4, lane 1, 5d). Given the similarity between muSP-DN cells and those reported perivascular primitive cells, muSP-DN cells would represent perivascular primitive mesenchymal cells in skeletal muscle.

Roles of muscle SP cells in muscle regeneration

muSP-DN cells actively proliferated and significantly increased in number upon muscle injury. The precise fate of muSP-DN cells has remained to be determined, since the number of muSP-DN cells returned to normal level at late stage of muscle regeneration.

We noted that angiogenic factors and TGF-β superfamily antagonists were strongly expressed in muSP-DN cells during muscle regeneration. Previous reports showed that *Ptc1*$^{+}$ interstitial mesenchymal cells in muscle produce angiogenic factors, including *ang1*, and promote muscle regeneration after ischemia [30,31]. Some members of the TGF-β superfamily, such as myostatin and TGF-β1, are known to act as negative regulators of myogenesis [32,33]. Inversely, one of the TGF-β superfamily antagonists, follistatin, has been reported to promote myoblast recruitment and fusion [34]. Therefore, muSP-DN cells might promote muscle regeneration by producing regeneration-regulating factors.

muSP-DN cells preferentially differentiate into myogenic cells after intramuscular transplantation, implying that normal muscle environment facilitates myogenic differentiation of muSP-DN cells. However, we revealed that muSP-DN cells have a high tendency to differentiate into osteogenic or adipogenic cells in vitro. Therefore, it is possible that muSP-DN cells differentiate into osteogenic or adipogenic cells in some pathological conditions such as Duchenne muscular dystrophy [35,36]. Recent finding that microvascular pericytes can differentiate into adipocytes [37] further supports the notion that muSP-DN cells might be implicated in pathological changes.

In conclusion, we identified novel subpopulation of muscle SP cells, CD31^{-} CD45^{-} SP cells, which possesses capacity of mesenchymal differentiation in vitro and reveals myogenic differentiation potential in vivo. Our findings might provide new insights that may well be useful in understanding adult skeletal muscle regeneration and in designing therapeutic strategies of muscular dystrophy.

Acknowledgments

The authors are grateful to Ms. A. Fukase for technical assistance, and colleagues in Department of Molecular Therapy, especially Dr. M. Imamura, for useful discussion and suggestions on this work. This work is supported by Grants-in-Aid for Center of Excellence (COE), Research on Nervous and Mental Disorders (13B-1, 16B-2), and Health Science Research Grants for Research on the Human Genome and Gene Therapy (H13-genome-001, H16-genome-003), for Research on Brain Science (H12-Brain-025, H15-Brain-021) from the Ministry of Health, Labor and Welfare, Grants-in-Aids for Scientific Research (14657158, 15390281, and 16590333) from the Ministry of Education, Culture, Sports, Science and Technology, and a Research Grant from National Space Development Agency of Japan (NASDA) and the Japan Space Forum.

Appendix A. Supplementary data

Supplementary data associated with this article can be found, in the online version, at doi:10.1016/j.bbrc.2006.01.037.

References

[1] R. Bischoff, Satellite and stem cells in muscle regeneration, in: A.G. Engel, C. Franzini-Armstrong (Eds.), Myology, McGraw-Hill, New York, 2004, pp. 66–86.
[2] G. Ferrari, G. Cusella-De Angelis, M. Coletta, E. Paolucci, A. Stornaiuolo, G. Cossu, F. Mavilio, Muscle regeneration by bone marrow-derived myogenic progenitors, Science 279 (1998) 1528–1530.
[3] M.A. Goodell, K. Brose, G. Paradis, A.S. Conner, R.C. Mulligan, Isolation and functional properties of murine hematopoietic stem cells that are replicating in vivo, J. Exp. Med. 183 (1996) 1797–1806.
[4] E. Gussoni, Y. Soneoka, C.D. Strickland, E.A. Buzney, M.K. Khan, A.F. Flint, L.M. Kunkel, R.C. Mulligan, Dystrophin expression in the mdx mouse restored by stem cell transplantation, Nature 401 (1999) 390–394.
[5] S. Fukada, Y. Miyagoe-Suzuki, H. Tsukihara, K. Yuasa, S. Higuchi, S. Ono, K. Tsujikawa, S. Takeda, H. Yamamoto, Muscle regener-

ation by reconstitution with bone marrow or fetal liver cells from green fluorescent protein-gene transgenic mice, J. Cell Sci. 115 (2002) 1285–1293.
[6] M.A. LaBarge, H.M. Blau, Biological progression from adult bone marrow to mononucleate muscle stem cell to multinucleate muscle fiber in response to injury, Cell 111 (2002) 589–601.
[7] F.D. Camargo, R. Green, Y. Capetanaki, K.A. Jackson, M.A. Goodell, Single hematopoietic stem cells generate skeletal muscle through myeloid intermediates, Nat. Med. 9 (2003) 1520–1527.
[8] S.L. McKinney-Freeman, S.M. Majka, K.A. Jackson, K. Norwood, K.K. Hirschi, M.A. Goodell, Altered phenotype and reduced function of muscle-derived hematopoietic stem cells, Exp. Hematol. 31 (2003) 806–814.
[9] A. Asakura, P. Seale, A. Girgis-Gabardo, M.A. Rudnicki, Myogenic specification of side population cells in skeletal muscle, J. Cell Biol. 159 (2002) 123–134.
[10] S.M. Majka, K.A. Jackson, K.A. Kienstra, M.W. Majesky, M.A. Goodell, K.K. Hirschi, Distinct progenitor populations in skeletal muscle are bone marrow derived and exhibit different cell fates during vascular regeneration, J. Clin. Invest. 111 (2003) 71–79.
[11] E. Bachrach, S. Li, A.L. Perez, J. Schienda, K. Liadaki, J. Volinski, A. Flint, J. Chamberlain, L.M. Kunkel, Systemic delivery of human microdystrophin to regenerating mouse dystrophic muscle by muscle progenitor cells, Proc. Natl. Acad. Sci. USA 101 (2004) 3581–3586.
[12] S. Fukada, S. Higuchi, M. Segawa, K. Koda, Y. Yamamoto, K. Tsujikawa, Y. Kohama, A. Uezumi, M. Imamura, Y. Miyagoe-Suzuki, S. Takeda, H. Yamamoto, Purification and cell-surface marker characterization of quiescent satellite cells from murine skeletal muscle by a novel monoclonal antibody, Exp. Cell Res. 296 (2004) 245–255.
[13] P. Seale, L.A. Sabourin, A. Girgis-Gabardo, A. Mansouri, P. Gruss, M.A. Rudnicki, Pax7 is required for the specification of myogenic satellite cells, Cell 102 (2000) 777–786.
[14] K. Ojima, A. Uezumi, H. Miyoshi, S. Masuda, Y. Morita, A. Fukase, A. Hattori, H. Nakauchi, Y. Miyagoe-Suzuki, S. Takeda, Mac-1^{low} early myeloid cells in the bone marrow-derived SP fraction migrate into injured skeletal muscle and participate in muscle regeneration, Biochem. Biophys. Res. Commun. 321 (2004) 1050–1061.
[15] J.D. Allen, R.F. Brinkhuis, J. Wijnholds, A.H. Schinkel, The mouse Berp1/Mxr/Abcp gene: amplification and overexpression in cell lines selected for resistance to topotecan, mitoxantrone, or doxorubicin, Cancer Res. 59 (1999) 4237–4241.
[16] T.A. Rando, H.M. Blau, Primary mouse myoblast purification, characterization, and transplantation for cell-mediated gene therapy, J. Cell Biol. 125 (1994) 1275–1287.
[17] Z. Qu, L. Balkir, J.C. van Deutekom, P.D. Robbins, R. Pruchnic, J. Huard, Development of approaches to improve cell survival in myoblast transfer therapy, J. Cell Biol. 142 (1998) 1257–1267.
[18] R. Kasturi, V.C. Joshi, Hormonal regulation of stearoyl coenzyme A desaturase activity and lipogenesis during adipose conversion of 3T3-L1 cells, J. Biol. Chem. 257 (1982) 12224–12230.
[19] S. Zhou, J.D. Schuetz, K.D. Bunting, A.M. Colapietro, J. Sampath, J.J. Morris, I. Lagutina, G.C. Grosveld, M. Osawa, H. Nakauchi, B.P. Sorrentino, The ABC transporter Berp1/ABCG2 is expressed in a wide variety of stem cells and is a molecular determinant of the side-population phenotype, Nat. Med. 7 (2001) 1028–1034.
[20] M. Maliepaard, G.L. Scheffer, I.F. Faneyte, M.A. van Gastelen, A.C. Pijnenborg, A.H. Schinkel, M.J. van De Vijver, R.J. Scheper, J.H. Schellens, Subcellular localization and distribution of the breast cancer resistance protein transporter in normal human tissues, Cancer Res. 61 (2001) 3458–3464.
[21] J.W. Jonker, M. Buitelaar, E. Wagenaar, M.A. Van Der Valk, G.L. Scheffer, R.J. Scheper, T. Plosch, F. Kuipers, R.P. Elferink, H. Rosing, J.H. Beijnen, A.H. Schinkel, The breast cancer resistance protein protects against a major chlorophyll-derived dietary photoxin and protoporphyria, Proc. Natl. Acad. Sci. USA 99 (2002) 15649–15654.
[22] F. Rivier, O. Alkan, A.F. Flint, K. Muskiewicz, P.D. Allen, P. Leboulch, E. Gussoni, Role of bone marrow cell trafficking in replenishing skeletal muscle SP and MP cell populations, J. Cell Sci. 117 (2004) 1979–1988.
[23] A.P. Meeson, T.J. Hawke, S. Graham, N. Jiang, J. Elterman, K. Hutcheson, J.M. Dimaio, T.D. Gallardo, D.J. Garry, Cellular and molecular regulation of skeletal muscle side population cells, Stem Cells 22 (2004) 1305–1320.
[24] S. Davis, T.H. Aldrich, P.F. Jones, A. Acheson, D.L. Compton, V. Jain, T.E. Ryan, J. Bruno, C. Radziejewski, P.C. Maisonpierre, G.D. Yancopoulos, Isolation of angiopoietin-1, a ligand for the TIE2 receptor, by secretion-trap expression cloning, Cell 87 (1996) 1161–1169.
[25] N. Takakura, T. Watanabe, S. Suenobu, Y. Yamada, T. Noda, Y. Ito, M. Satake, T. Suda, A role for hematopoietic stem cells in promoting angiogenesis, Cell 102 (2000) 199–209.
[26] M.J. Doherty, B.A. Ashton, S. Walsh, J.N. Beresford, M.E. Grant, A.E. Canfield, Vascular pericytes express osteogenic potential in vitro and in vivo, J. Bone Miner. Res. 13 (1998) 828–838.
[27] M.M. Levy, C.J. Joyner, A.S. Virdi, A. Reed, J.T. Triffitt, A.H. Simpson, J. Kenwright, H. Stein, M.J. Francis, Osteoprogenitor cells of mature human skeletal muscle tissue: an in vitro study, Bone 29 (2001) 317–322.
[28] S. Shi, S. Gronthos, Perivascular niche of postnatal mesenchymal stem cells in human bone marrow and dental pulp, J. Bone Miner. Res. 18 (2003) 696–704.
[29] M. Iurlaro, M. Scatena, W.H. Zhu, E. Fogel, S.L. Wieting, R.F. Nicosia, Rat aorta-derived mural precursor cells express the Tie2 receptor and respond directly to stimulation by angiopoietins, J. Cell Sci. 116 (2003) 3635–3643.
[30] R. Pola, L.E. Ling, M. Silver, M.J. Corbley, M. Kearney, R. Blake Pepinsky, R. Shapiro, F.R. Taylor, D.P. Baker, T. Asahara, J.M. Isner, The morphogen Sonic hedgehog is an indirect angiogenic agent upregulating two families of angiogenic growth factors, Nat. Med. 7 (2001) 706–711.
[31] R. Pola, L.E. Ling, T.R. Aprahamian, E. Barban, M. Bosch-Marce, C. Curry, M. Corbley, M. Kearney, J.M. Isner, D.W. Losordo, Postnatal recapitulation of embryonic hedgehog pathway in response to skeletal muscle ischemia, Circulation 108 (2003) 479–485.
[32] Y. Li, W. Foster, B.M. Deasy, Y. Chan, V. Prisk, Y. Tang, J. Cummins, J. Huard, Transforming growth factor-beta1 induces the differentiation of myogenic cells into fibrotic cells in injured skeletal muscle: a key event in muscle fibrogenesis, Am. J. Pathol. 164 (2004) 1007–1019.
[33] A.C. McPherron, A.M. Lawler, S.J. Lee, Regulation of skeletal muscle mass in mice by a new TGF-beta superfamily member, Nature 387 (1997) 83–90.
[34] S. Iezzi, M. Di Padova, C. Serra, G. Caretti, C. Simone, E. Maklan, G. Minetti, P. Zhao, E.P. Hoffman, P.L. Puri, V. Sartorelli, Deacetylase inhibitors increase muscle cell size by promoting myoblast recruitment and fusion through induction of follistatin, Dev. Cell 6 (2004) 673–684.
[35] A.G. Engel, E. Ozawa, Dystrophinopathies, in: A.G. Engel, C. Franzini-Armstrong (Eds.), Myology, McGraw-Hill, New York, 2004, pp. 961–1025.
[36] B.Q. Banker, A.G. Engel, Basic reactions of muscle, in: A.G. Engel, C. Franzini-Armstrong (Eds.), Myology, McGraw-Hill, New York, 2004, pp. 691–747.
[37] C. Farrington-Rock, N.J. Crofts, M.J. Doherty, B.A. Ashton, C. Griffin-Jones, A.E. Canfield, Chondrogenic and adipogenic potential of microvascular pericytes, Circulation 110 (2004) 2226–2232.

Acta Myologica • 2005; XXIV: p. 134-144

ORIGINAL ARTICLES

Intracellular Localization of Dysferlin and its Association with the Dihydropyridine Receptor

BERYL N. AMPONG[1,2], MICHIHIRO IMAMURA[1], TERUHIRO MATSUMIYA[2], MIKIHARU YOSHIDA[1] AND SHIN'ICHI TAKEDA[1]

[1]*Department of Molecular Therapy, National Institute of Neuroscience, National Center for Neurology and Psychiatry, 4-1-1 Ogawahigashi-cho, Kodaira, Tokyo 187-8502, Japan*

[2]*Department of Pharmacology, Tokyo Medical University, 6-1-1 Shinjuku, Tokyo 160-8402, Japan*

Mutations in the *dysferlin* gene underlie two phenotypically distinct muscular dystrophies: Miyoshi myopathy and limb-girdle muscular dystrophy 2B. Dysferlin was proposed to have a putative functional role in mediating the fusion of intracellular vesicles to the sarcolemma during injury-induced membrane repair, but dysferlin has been found not only at the sarcolemma but also within the cytoplasm of skeletal muscle fibers by immunohistochemistry. In this study, we examined the subcellular localization of dysferlin in skeletal muscle by immunohistochemical and biochemical analyses to elucidate other functional roles of dysferlin. Immunohistochemistry confirmed granular cytoplasmic expression pattern of dysferlin in muscle fibers. Subcellular membrane fractionation revealed that a portion of dysferlin associated with a T-tubule-enriched intracellular membrane fraction as well as a sarcolemmal fraction. This indication was consistent with subsequent results that dysferlin coprecipitates by immunoprecipitation with the dihydropyridine receptor (DHPR), a protein complex localized in T-tubules. Moreover, both proteins were observed to partially colocalize by double immunofluorescent labeling in skeletal muscle fibers. We also found that caveolin-3, previously shown to interact with dysferlin, coprecipitates with DHPR. These results demonstrated that dysferlin may be involved in the formation of an oligomeric complex with DHPR and caveolin-3. Caveolin-3 has been also reported to participate in an insulin-regulated transport mechanism in muscle, and caveolin-3-containing vesicles might traffic between intracellular sites and target sites on the sarcolemma and T-tubules. Therefore, it is very intriguing to assume that dysferlin might be involved in the fusion of caveolin-3-containing vesicles with T-tubules.

Key Words: dysferlin, T-tubules, caveolin-3

Introduction

Two phenotypically distinct forms of muscular dystrophy with autosomal recessive inheritance, Miyoshi myopathy and limb girdle muscular dystrophy 2B (LGMD 2B) are reported to be caused by genetic mutations in the *dysferlin* gene (*DYSF*). Distal or proximal muscles are known to be predominantly involved in Miyoshi myopathy or in LGMD 2B, respectively [1,2]. Both diseases are clinically characterized by a late onset and slow progression of symptoms, as well as elevated serum creatine kinase levels [3]. *DYSF* was identified through positional cloning and mapped to the 2p13 gene locus [4,5]. It consists of over 55 exons transcribed into an 8.5 kb major transcript predominantly expressed in skeletal muscle [4,5].

The functional role of dysferlin in muscle physiology and pathology has been the subject of extensive research over the years. Studies of its cDNA sequence predict a protein of approximately 230 kDa, typically a type II transmembrane protein. Dysferlin contains sequences of calcium-binding C2 domains. These are motifs found in a number of proteins involved in signal transduction and membrane trafficking [6] such as the calcium-sensing synaptotagmins [7] and protein kinase C [8]. In addition, dysferlin has recently been identified as a member of a unique family of proteins: the ferlins. These proteins, which include myoferlin [9] and otoferlin [10], have as an important functional characteristic a high sequence homology to the *C. elegans* fer-1 protein, reported to play a critical role in the fusion of intracellular vesicles with the plasma membrane in sperm cells [11]. This has suggested a putative role for dysferlin in mediating the fusion of intracellular vesicles with the sarcolemma of skeletal muscle fibers in a calcium-dependent manner. Indeed, dysferlin knockout mice developed a slowly progressive muscular dystrophy due to an inability of intracellular vesicles

Address for correspondence: Mikiharu YOSHIDA, Department of Molecular Therapy, National Institute of Neuroscience, NCNP, 4-1-1 Ogawahigashi-cho, Kodaira, Tokyo 187-8502, Japan

to fuse with the sarcolemma during injury-induced membrane repair [12]. The fusion process has also been suggested to involve an interaction between dysferlin and the annexins; calcium and phospholipid-binding proteins implicated in membrane repair [13]. The presence of dysferlin has been shown not only at the sarcolemma [12-16] but also within the cytoplasm [12,16] of skeletal muscle fibers by immunohistochemistry and it has been proposed that dysferlin present on the intracellular vesicles is involved in the injury-induced fusion process [17].

In the present study, we systematically examined the localization of dysferlin in the muscle fiber by immunohistochemical and biochemical analyses in order to characterize the intracellular localization of dysferlin. Our immunohistochemical results confirmed the presence of dysferlin at the sarcolemma and within the cytoplasm of muscle fibers. In membrane fractionation experiments, dysferlin was shown to be associated with a T-tubule-enriched intracellular membrane fraction in addition to a sarcolemmal fraction. This association with a T-tubule-enriched membrane fraction was consistent with subsequent results shown by immunoprecipitation experiments that dysferlin coprecipitates with the dihydropyridine receptor (DHPR), a protein complex localized in T-tubules. We also found that caveolin-3, previously shown to interact with dysferlin, coprecipitates with DHPR by immunoprecipitation.

Materials and methods

Animals

Wistar rats and mice (Balb/c and SJL) were purchased from Clea Japan Inc. (Tokyo, Japan) and Charles River Japan Inc. (Tokyo, Japan) respectively. The SJL mouse is a naturally occurring animal model of dysferlin deficiency caused by an inframe deletion mutation in the *dysferlin* gene. It has been shown that expression of truncated dysferlin is greatly reduced [18,19] in skeletal muscles of this animal model. All animal handling procedures were performed in accordance with protocols approved by the National Institute of Neuroscience, NCNP, Kodaira, Japan.

Antibodies

For immunoprecipitation studies, a polyclonal antibody against dysferlin was raised by immunizing rabbits with a polypeptide corresponding to the amino acid sequence of human dysferlin 1999 to 2016 conjugated with keyhole limpet hemocyanin, and emulsified with the adjuvant TiterMax Gold (CytRx Corp., Atlanta, GA). The antiserum was affinity-purified by absorption onto a polypeptide coupled to thiopropyl-Sepharose 6B (Amersham Biosciences Corp., Piscataway, NJ) followed by elution with 4 M $MgCl_2$. In immunoblot analysis, the antibody specifically reacted with dysferlin in microsomes of mouse skeletal muscle (data not shown). Monoclonal antibodies against dysferlin (NCL-Hamlet) and dystrophin (NCL-DYS2) were purchased from Novocastra Laboratories Ltd Newcastle, UK. Polyclonal antibody against α-actinin was obtained as described [20]. Antibodies against triadin, DHPR (α2 subunit), ryanodine receptor and sarco/endoplasmic reticulum calcium ATPase1 (SERCA1) were obtained from Affinity Bioreagents, Inc. (Golden, CO). Antibodies against NaK-ATPase α1 and DHPR subunit α1 were obtained from Upstate Biotech (Lake Placid, NY). Monoclonal antibodies against annexin A2 and caveolin-3 were from BD Transduction Labs. (San Jose, CA). Anti-NSF antibody was from ICN Biomedicals, Inc. (Aurora, OH). Anti-desmin antibody was from Progen Biotechnik GMBH (Heidelberg, Germany). Goat polyclonal antibodies against DHPR α1, SERCA1 and caveolin-3 were from Santa Cruz Biotech., Inc. (Santa Cruz, CA). The Alexa-conjugated secondary antibodies were purchased from Molecular Probes Inc. (Eugene, OR).

Immunohistochemical analysis

Animals were killed by CO_2 inhalation followed by cervical dislocation. Tibialis anterior (TA) muscles were rapidly dissected out and snap-frozen in liquid nitrogen-cooled isopentane. 6 μm thick cryostat sections were fixed by immersion in 4% paraformaldehyde in phosphate-buffered saline (PBS), pH 7.4, at 4°C for 2 min, dehydrated in 70% ethanol at 4°C for 10 min and then permeated with 0.1% triton X-100 in PBS at room temperature for 10 min. Sections were washed and incubated for 25 s with proteinase K solution (550 U/ml, Wako Pure Chemical Industries Ltd, Osaka, Japan) at a dilution of 1:300 in TE buffer [10 mM Tris-HCl (pH 8.0), 1 mM EDTA]. After washing, sections were incubated in primary antibody diluted in 2% casein in PBS at 4°C overnight. For double immunostaining, sections were incubated overnight in a mixture of the relevant primary antibodies diluted in 2% casein in PBS. After primary

antibody incubation, sections were washed three times for 5 min with PBS and then incubated for 1 h with the relevant secondary antibodies. After washing, sections were mounted in VectaShield® mounting medium (Vector Labs, Burlingame, CA) and coverslipped. Fluorescent images were captured by confocal-laser scanning microscope (Leica TCS SP, Leica, Heidelberg, Germany)

Subcellular membrane fractionations

Two different subcellular membrane fractionation protocols were used in the present study. The first protocol used (Fig 2A) was a slight modification of that previously reported by Dombrowski *et al* [21]. Briefly, muscles (~1 g) were excised from the hindlimbs of mice, cut into small pieces with scissors and frozen in liquid nitrogen. The frozen muscles were pulverized by the use of Cryo-Press chilled with liquid nitrogen and homogenized at 4°C with Polytron PT3000 equipped with a DA 3012/2S probe (Kinematica, AG, Littau Lucerne, Switzerland) at 16,000 rpm for 10 s. The original homogenizing buffer was changed to buffer A containing 20 mM sodium pyrophosphate, 20 mM sodium phosphate, 0.25 M sucrose, 0.5 mM O, O'-bis(2-aminoethyl)ethyleneglycol-N, N, N', N'-tetraacetic acid and 1 mM $MgCl_2$ (pH 7.1) in order to decrease non-specific aggregation. Discontinuous sucrose density gradient centrifugation experiments were omitted in this study.

In the second protocol (Fig 3A), sarcolemma was purified by the method of Munoz *et al* [22]. Homogenization steps were slightly modified as follows. Freshly dissected mouse hindlimb muscles (~6 g) were homogenized twice with a Polytron homogenizer (PT3000) at 4°C, 13,000 rpm for 20 s and centrifuged. The pellet was resuspended and again homogenized twice with the Polytron homogenizer at 17,000 rpm for 30 s. After centrifugation, the two supernatants were pooled and the remaining procedures were carried out in accordance with Munoz *et al*. Protease inhibitor cocktail, complete EDTA free (Roche Diagnostics GmbH, Mannheim, Germany) was included in all buffers used. All other reagents were purchased from Wako Pure Chemical.

Fractionation of microsomal proteins

Fractionation of digitonin-solubilized microsomes from rabbit skeletal muscle by wheat-germ agglutinin (WGA) gel chromatography was performed as previously described [23].

Immunoprecipitation

Besides anti-dysferlin antibody prepared in this study, anti-DHPR α1 (Upstate Biotech), anti-DHPR α2 and anti-caveolin-3 (Santa Cruz) antibodies were used for immunoprecipitation. Each IgG was coupled with the gel by use of Affi-Gel Hz immunoaffinity kit (Bio-Rad Labs, Hercules, CA). Prepared gels were washed once before use with the elution buffer: 0.15 M glycine-HCl, pH 2.5 and 0.1% digitonin before use. The WGA-bound microsomal proteins were mixed with approximately 50 μl of the gel equilibrated with the binding buffer: 0.15 M NaCl, 20 mM Hepes-NaOH, 0.1% digitonin, protease inhibitor cocktail Complete EDTA-free (Roche Diagnostics GmbH) in a MicroSpin column (Amersham Biosciences) and incubated overnight at 4°C with gentle agitation. The gel in the column was then washed many times with the binding buffer and eluted with the elution buffer. Washing and eluting procedures were performed by gravity drip from the column. The eluted proteins were neutralized with 2 M Tris-HCl, pH 9.0 and ultrafiltrated close to dehydration with Microcon 30 (Millipore Corp., Bedford, MA). The proteins were extracted from the membrane with the buffer containing 1% SDS, 1 mM TCEP (Pierce Biotechnology Inc., Rockford, IL) and 22 mM Tris-HCl (pH 6.7), and concentrated to one-third volume with a centrifugation evaporator.

Protein concentration was determined by Protein Assay Stain (Bio-Rad) or Coomassie Plus-200 Protein Assay Reagent (Pierce Biotechnology) using either BSA or γ-globulin as a standard.

Electrophoresis and Immunoblot Analysis

In SDS-PAGE, proteins were run on 5-10% or 5-15% precast gel (DRC, Tokyo, Japan). Subsequent transfer from the gel on to PVDF membranes (Millipore) was performed for 1 h at a current of 5 mA/cm^2 with a buffer similar to that of Kyhse-Anderson [24]. Following transfer, membranes were blocked with PBS including each 0.1% of casein and gelatin for 1 h at room temperature, and then incubated with primary antibodies followed by the respective horse-radish-peroxidase (HRP)-labeled secondary antibodies. Molecular masses were estimated with Biotinylated Standards kit (Bio-Rad) and HRP-labeled avidin. Bound antibodies were detected by chemiluminescence with Supersignal West Dura Extended Duration Substrate (Pierce Biotechnology). Signals were visualized with Luminoimager (Roche Diagnostics). Blot overlay assay for the

WGA-binding proteins was performed in accordance with the method of Yoshida and Ozawa [23]. Bound biotinyl WGA was detected with a combination of an RTU Vectastain Elite ABC reagent and a VIP-staining kit (Vector Labs).

Results

Immunohistochemical analysis of dysferlin in skeletal muscle fibers

We first analyzed the localization of dysferlin in skeletal muscles of Wistar rats and Balb/c mice by confocal laser-scanning microscopy. In both transverse and longitudinal cryosections, a mouse monoclonal antibody against dysferlin stained not only the sarcolemma but also the cytoplasm of muscle fibers (Fig. 1). In transverse sections, the cytoplasmic staining was observed as a granular staining pattern that appeared intense in some fibers. This staining pattern is similar to that previously reported [12]. In longitudinal sections, cytoplasmic localization was observed as cross-striated double bands under high magnification. We found no correlation between the intense cytoplasmic staining observed in some fibers and fiber type distribution (data not shown). We also examined the localization of dysferlin in skeletal muscles of SJL mice, which have an inframe deletion in the *dysferlin* gene. Dysferlin staining was significantly reduced from the sarcolemma and cytoplasm in both transverse and longitudinal sections of SJL mice skeletal muscle (Fig. 1). To investigate the specificity of the fluorescence signals observed, the antibody was also incubated with a polypeptide corresponding to its epitope. This resulted in a loss of any signal in the muscle sections (data not shown). These results indicate that dysferlin is localized not only on the sarcolemma but also within the cytoplasm of muscle fibers.

Subcellular distribution of dysferlin

Next, we examined the localization of dysferlin within muscle fibers by biochemical fractionation, using a previously established procedure [21] (Fig. 2A). This protocol allowed for the isolation of three distinct membrane fractions; a crude microsomal fraction enriched in sarcolemmal membranes (F2), and two internal membrane fractions: PF4 enriched in T-tubule and SR membranes, and PF8 an intracellular pool for glucose transporter4 (Glut4).

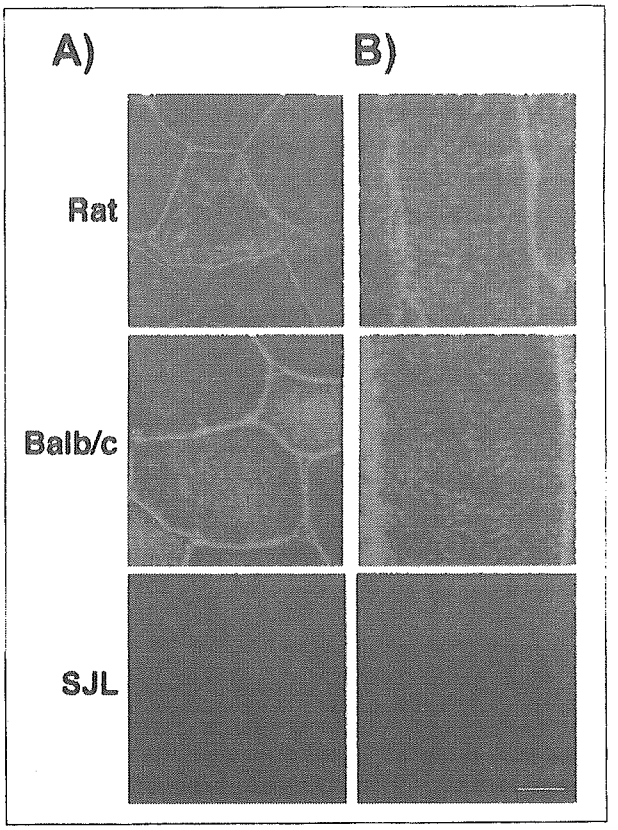

Fig. 1. Immunohistochemical analysis of dysferlin in skeletal muscle fibers. A) and B), immunofluorescent images of transverse and longitudinal sections (6 µm), respectively, of the tibialis anterior (TA) muscles of Wister rats, Balb/c and SJL mice stained with monoclonal antibody against dysferlin. Scale bar, 20 µm.

Fractions obtained from Balb/c and SJL mice were analyzed for dysferlin and a number of other protein markers (Fig. 2B). NaK-ATPase, a sarcolemmal marker, was detected only in the F2 fraction. This fraction also included annexin A2 [13] and caveolin-3 [25], two proteins reported to interact with dysferlin at the sarcolemma. On the other hand, the PF4 fraction contained the intracellular membrane proteins DHPR, SERCA1, triadin and the ryanodine receptor, although some amounts of these were also detected in the F2 fraction. As shown in Fig. 2B, dysferlin was detected not only in the sarcolemma-enriched F2 fraction, but also in the PF4 fraction. Furthermore, the intensity of the dysferlin signal was found to be similar between F2 and PF4. This result shows that a substantial amount of dysferlin distinctly associates with non-sarcolemmal membranes.

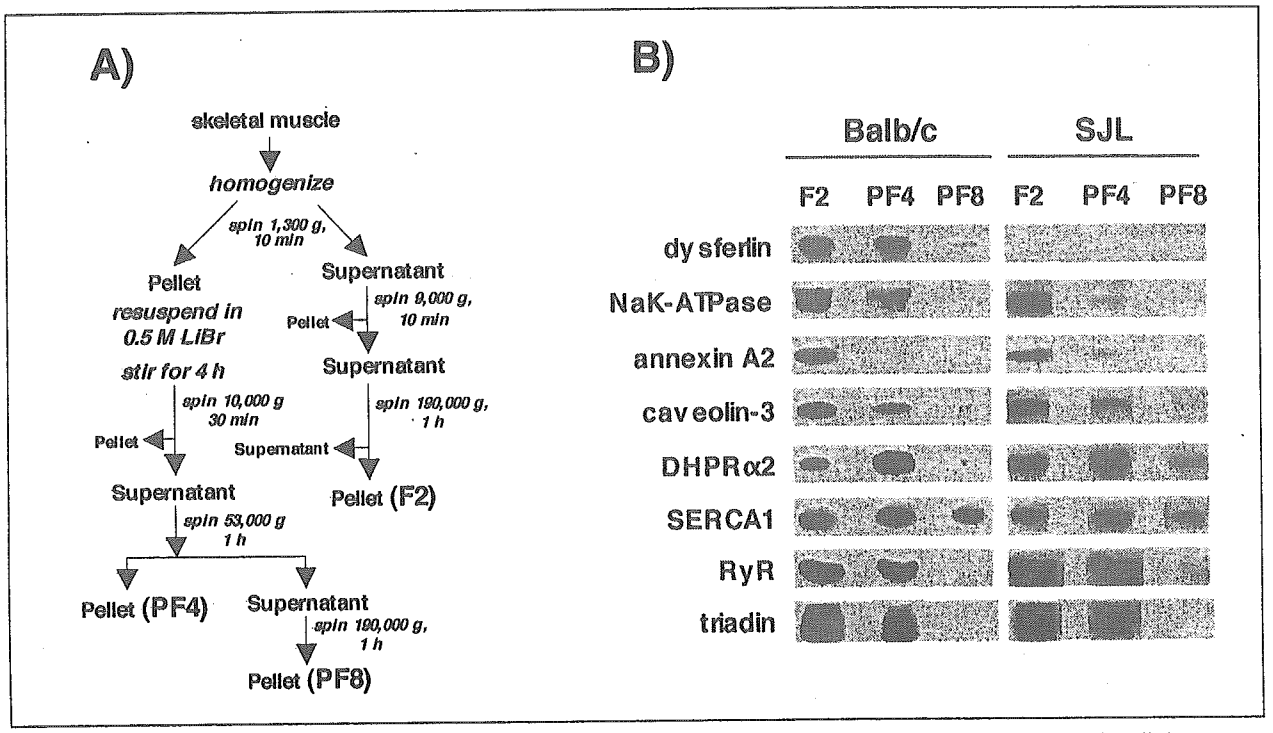

Fig. 2. Subcellular distribution of dysferlin in skeletal muscle. A) Schematic representation of subcellular membrane fractionation protocol [21]. F2, a crude microsomal fraction enriched in sarcolemmal membranes; PF4, internal membrane fraction enriched in T-tubule and SR membranes; PF8, internal membrane fraction enriched in GLUT4-containing intracellular membranes. B) Immunoblot analysis of the fractions obtained from Balb/c and SJL mice. Membrane proteins of each fraction were loaded on the respective lanes in equal amounts, although the amount was changed depending on the antibody used for analysis (0.05 to 5 μg). Dysferlin was detected in fractions F2 and PF4, but not in PF8. RyR, ryanodine receptor.

In the analysis of SJL mice, dysferlin was undetectable. However, we did not observe any significant changes in the amount or distribution of the other marker proteins analyzed (Fig. 2B).

Close association of dysferlin with T-tubules

The subcellular fractionation data demonstrated the presence of dysferlin in membrane fractions enriched in T-tubules and SR (Fig. 2). To further clarify the association of dysferlin with these internal membranes, we extracted crude microsomes from mouse skeletal muscle homogenates using a protocol first described by Munoz et al [22]. This crude microsomal preparation, obtained under physiological condition, includes internal membranes. This was then separated into 4 fractions based on individual densities (Fig. 3A). The lightest of these, 23F, is reportedly a fraction enriched in sarcolemma and T-tubule membranes. 26F and 29F are enriched in intracellular Glut4-containing vesicles and 35F is essentially an SR-enriched fraction [22]. Immunoblot analysis (Fig. 3B) showed that the sarcolemmal marker, NaK-ATPase was mainly recovered in 23F, with trace amounts detected in 26F. The N-ethylmaleimide-sensitive fusion protein (NSF), a chaperone required for the fusion of transport vesicles to their target membranes [26], displayed a similar distribution pattern to that of NaK-ATPase. SERCA1 was mainly detected in 35F and to a lesser extent in 29F, meaning most of the SR was recovered in these fractions. The T-tubule marker DHPR was detected in all fractions in the present experiment. This contrasts with the results of Munoz et al [22]. This discrepancy may be due to species differences between mice and rats. Dysferlin was mostly detected in 23F and 26F, with lesser amounts detected in 29F. The near absence of dysferlin in the SR-enriched fraction (35F) suggests that it is not likely associated with SR membranes. Caveolin-3, a dysferlin-interacting protein, was detected in fractions 23F, 26F and 29F.

Further fractionation of 23F by WGA agglutination allows for the separation of a pure sar-

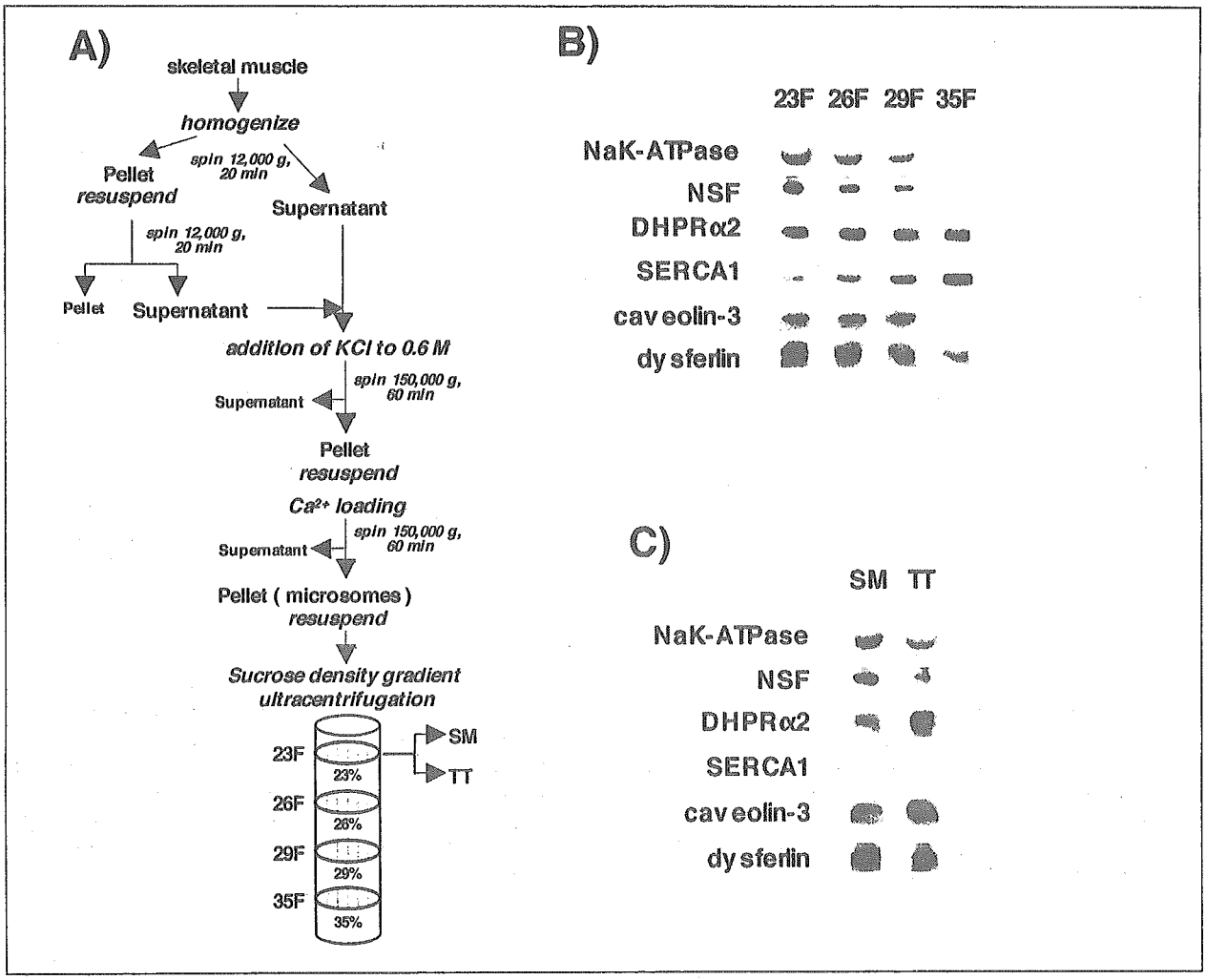

Fig. 3. Close association of dysferlin with T-tubules. A) Schematic representation of microsomal membrane fractionation protocol [22]. 23F; light microsomal fraction enriched in sarcolemmal and T-tubule membranes, 26F and 29F; fractions enriched in Glut4-containing intracellular vesicles, 35F; an SR-enriched fraction. SM and TT; the subfractions of 23F that were agglutinated and non-agglutinated with WGA, respectively. B) Immunoblot analysis of the four microsomal fractions with various antibodies. Membrane proteins in each fraction were loaded on the respective lanes in equal amounts, with the amounts changing depending on the antibody used (0.3 to 6 μg). Dysferlin was detected in 23F and 26F, and to a lesser extent in 29F. C) Immunoblot analysis of SM and TT fractions with various antibodies. The amount of dysferlin was similar between both fractions.

colemmal fraction (SM) from a T-tubule-enriched membrane fraction (TT) [22]. This is based on the principle that WGA receptors present on T-tubules cannot interact with WGA, because of the inside-out orientation of the fragmented T-tubular membrane. As shown in Fig. 3C, NaK-ATPase and NSF were mainly detected in the SM fraction, while DHPR was mostly detected in the TT fraction. SERCA1 was notably absent from both fractions. Interestingly, dysferlin was recovered in similar amounts in both SM and TT, demonstrating that in addition to sarcolemmal localization, dysferlin closely associates with T-tubule membranes. Caveolin-3 was also detected in both fractions but comparatively more in TT.

Interaction of dysferlin with DHPR

To date, dysferlin has been reported to interact with annexins A1 & A2 [13], caveolin-3 [25] and affixin [27]. The presence of dysferlin in T-tubule-enriched intracellular membrane fractions suggests the possibility of other dysferlin-interacting proteins.

To investigate this possibility, we solubilized crude microsomes with digitonin and fractionated them using WGA gel affinity chromatography as depicted in Fig. 4A. As expected, dystrophin [28] and DHPR [29] were detected in the bound fraction, and proteins such as SERCA1 and NSF were detected in the flow-through fraction (Fig. 4B). Interestingly, dysferlin was detected in both fractions, indicating that a portion of dysferlin was bound to WGA. Since the amino acid sequence of dysferlin precludes it as a glycoprotein [4,5], this finding suggested to us that a portion of dysferlin may bind to WGA probably through an association with WGA-binding protein(s). Caveolin-3 was also detected in both fractions.

To find out which WGA-binding protein(s) may associate with dysferlin, we immunoprecipitated dysferlin from the bound fraction and examined the precipitate for the presence of WGA-binding protein(s). Since the anti-dysferlin monoclonal antibody hitherto used was not suitable for immunoprecipitation, we raised an anti-dysferlin polyclonal antibody in rabbits as described under materials and methods. This polyclonal antibody specifically reacted with dysferlin in skeletal muscle membranes of mice (data not shown). Using this antibody, an immunoprecipitate was prepared from the WGA-bound fraction and analyzed by blot overlay assay with biotinyl WGA. As shown in Fig. 4C, positive bands were detected at approximately the 80-, 100- and 140-kDa positions. We predicted these to be putative dysferlin-interacting proteins.

DHPR, shown to bind to the WGA gel (Fig. 4B), is a protein complex composed of four subunits; α1, α2, β and γ. It reportedly binds to the gel through its

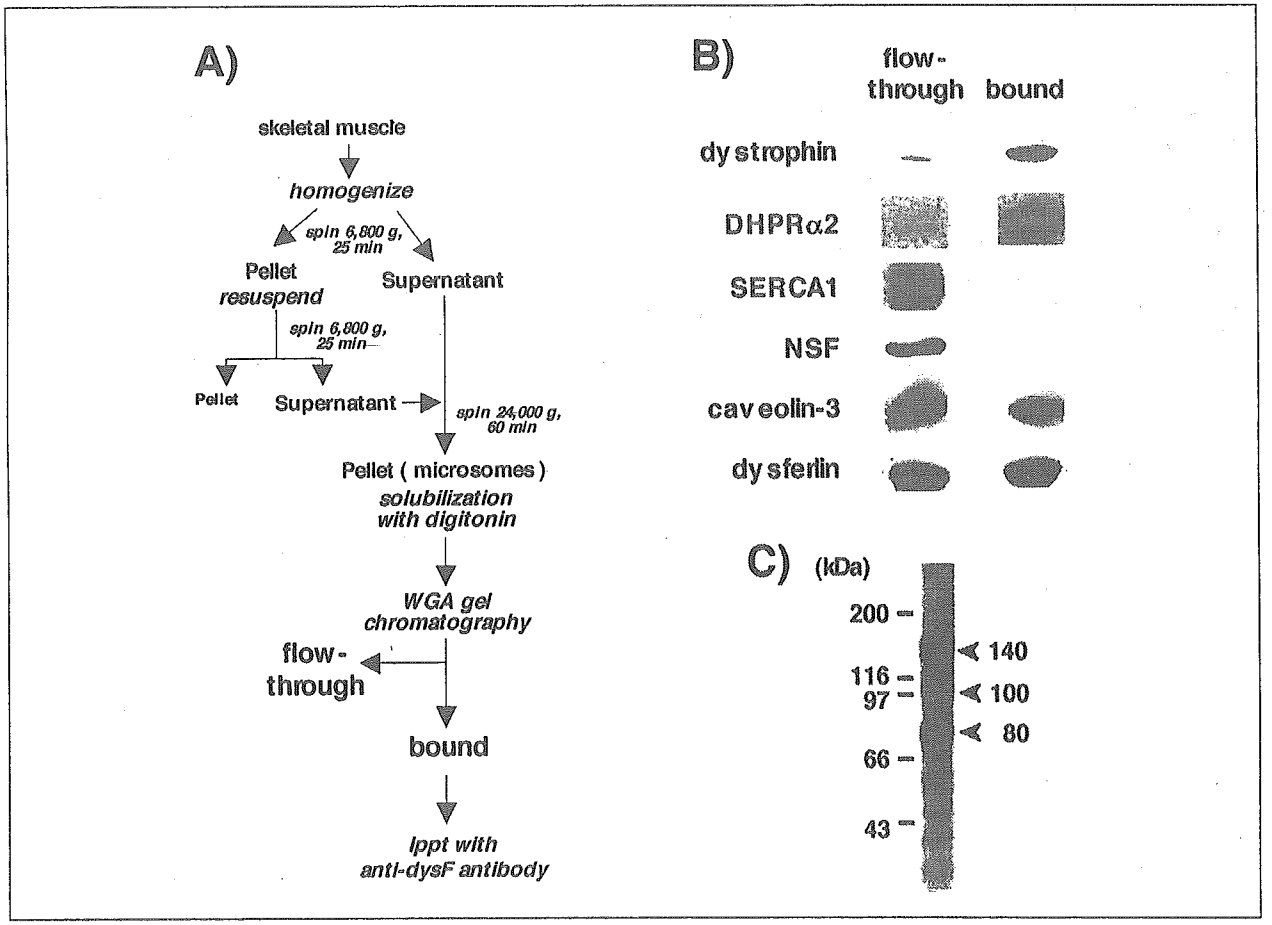

Fig. 4. Investigation of dysferlin-binding proteins. A) Schematic representation of crude microsome preparation and WGA gel chromatography of digitonin-solubilized microsomal proteins. B) Immunoblot analysis of the flow-through and bound fractions with various antibodies. The volume of both fractions was adjusted and aliquots loaded onto the gel. C) Blot overlay assay with biotinyl WGA of the immunoprecipitate prepared from the WGA-bound fraction with anti-dysferlin polyclonal antibody. Proteins of approximate molecular masses 140, 100 and 80 kDa were shown to react with WGA.

α2 subunit [29]. Its molecular mass of approximately 140 kDa under reduced conditions [29] is consistent with that of the largest dysferlin-interacting protein we detected (Fig. 4C). To test the possibility that dysferlin may associate with the WGA gel through an association with DHPR, we performed a series of immunoprecipitation experiments using the WGA-bound fraction. As shown in Fig. 5, DHPR was immunoprecipitated by an anti-dysferlin antibody, and conversely, dysferlin was immunoprecipitated by anti-DHPR α1 and α2 antibodies. This clearly demonstrates an interaction between dysferlin with DHPR. In another group of experiments we confirmed the presence of the dysferlin-interacting protein, caveolin-3 in immunoprecipitates prepared using the anti-dysferlin antibody. Additionally, analysis of immunoprecipitates prepared with both anti-DHPR α1 and α2 antibodies demonstrated the presence of caveolin-3, while anti-caveolin-3 antibody was found to reciprocally immunoprecipitate DHPR. These results suggest an association between DHPR and caveolin-3. Relative amounts of caveolin-3 in immunoprecipitation study indicated that only a portion of caveolin-3 might participate in the complex with dysferlin and DHPR.

We have not identified the 100- and 80-kDa WGA-binding proteins that were shown to interact with dysferlin, but their presence indicates that dysferlin may interact with more proteins than presently known.

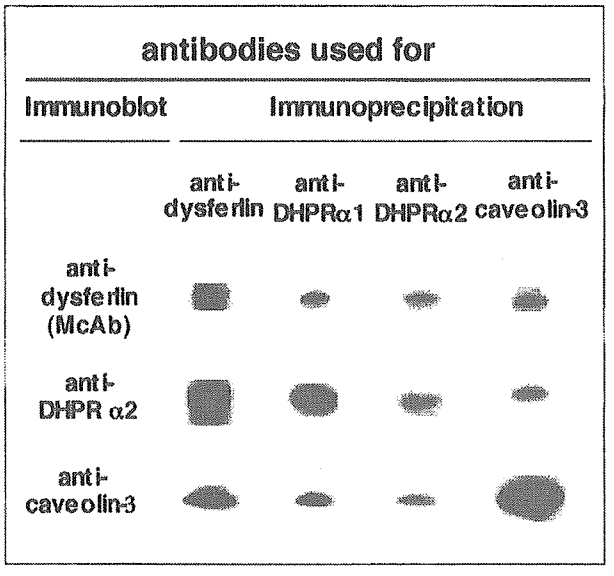

Fig. 5. Dysferlin, DHPR and caveolin-3 mutually interact. Immunoblot analysis of immunoprecipitates prepared from WGA-bound microsomal proteins. One μl of immunoprecipitates was loaded on each lane.

Partial colocalization of dysferlin with DHPR

Based on our finding that dysferlin interacts with DHPR and caveolin-3, we expect that these proteins would colocalize in skeletal muscle fibers. Therefore we set out to verify this by double immunofluorescent staining. The anti-dysferlin monoclonal and anti-DHPR α1 antibodies both produced cross-striated bands of dysferlin and DHPR, respectively, in longitudinal sections of skeletal muscle fibers (Fig. 6). Analysis of double stained patterns revealed areas of colocalization between the two proteins.

Anti-caveolin-3 antibody showed a less organized cytoplasmic staining pattern in comparison with dysferlin and DHPR, and double staining did not show clear colocalization between caveolin-3 and either DHPR (data not shown) or dysferlin. This might be explained by the notion that only a small portion of caveolin-3 associated with DHPR and dysferlin, as suggested by immunoprecipitation.

We also investigated the localization of dysferlin in relation to other well characterized sarcomeric protein markers such α-actinin and desmin, two functionally different proteins associated with Z-

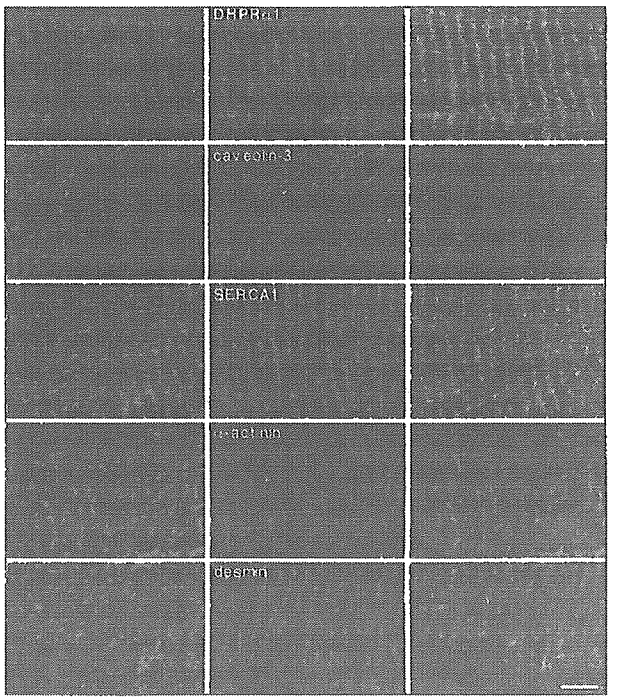

Fig. 6. Partial colocalization of dysferlin and DHPR. High-resolution images of 6 μm longitudinal sections from the TA muscle of Wistar rats double stained with monoclonal antibody against dysferlin (red, left panels) and antibodies against DHPR α1, caveolin-3, SERCA1, α-actinin and desmin (green, center panels). Respective merged images are shown on the right panels. Scale bar, 5 μm.

lines, and SERCA1, a protein responsible for the uptake of calcium into intracellular stores. Double staining of dysferlin with either α-actinin or desmin showed no areas of colocalization. Instead, striations produced by either α-actinin or desmin were labeled within the dysferlin doublet striated pattern. Results with SERCA1 were similar to that obtained with DHPR, with comparatively fewer areas of colocalization observed.

Discussion

While no comprehensive report has been published detailing the precise localization of dysferlin within the muscle fiber, a careful examination of literature shows a consensus indicating the presence of dysferlin at both the sarcolemma [12-16] and within the cytoplasm [12,16] of muscle fibers. In the present study we confirmed the presence of dysferlin at the sarcolemma initially by immunohistochemical observation (Fig. 1). Subsequent biochemical analysis revealed the presence of dysferlin, first in a crude microsomal fraction (Fig. 2), and then in a pure sarcolemmal fraction prepared from light microsomes (Fig. 3). We also observed dysferlin localization as granular cytoplasmic staining within muscle fibers by immunohistochemistry (Fig. 1). This pattern of cytoplasmic localization was of interest in view of the fact that dysferlin has a putative role in mediating intracellular vesicle fusion with the sarcolemma [12,13]. However, since not much is known about the nature of this intracellular localization, we investigated this further via a series of biochemical experiments.

Two significant findings were made in this study. The first of these was the observation that in addition to the pure sarcolemmal fraction, a portion of dysferlin was present in a T-tubule-enriched intracellular membrane fraction (Fig. 3). This was determined using a protocol of subcellular fractionation with further purification by WGA agglutination. T-tubules are specialized membrane invaginations of the sarcolemma and carry membrane depolarization deep into the fiber to trigger excitation-contraction coupling [30]. The protein and lipid composition of this system has been shown to be very distinct from that of the sarcolemma [30]. This suggests that the association of dysferlin with T-tubules may be independent of its localization at the sarcolamma, and is the first published data describing an association of dysferlin with non-sarcolemmal membranes.

Another significant finding was the identification of DHPR as a dysferlin-interacting protein complex. This result supports the finding of dysferlin present on T-tubules. The DHPR is responsible for the L-type Ca^{2+} current and serves as the voltage sensor for excitation contraction coupling [32]. It is composed of α1, α2, β and γ subunits [29]. The α1 subunit is a transmembrane protein that contains the basic functional elements for the L-type Ca^{2+} channel while the β subunit is an intracellular protein essential for excitation contraction coupling. The functional significance of the α2 and γ subunits is not clearly defined [32].

The question remains as to exactly how dysferlin associates with DHPR. Two possibilities exist as to how dysferlin may interact with DHPR. One involves a lateral association between dysferlin and DHPR in T-tubule membranes. The other involves an association between dysferlin, present in intracellular vesicles, and DHPR. Double immunostaining (Fig. 6) and membrane fractionation experiments indicate that the entire DHPR complex may not interact with dysferlin. Therefore, we are of the opinion that the interaction occurs between dysferlin and DHPR present on distinct membranes respectively.

It is not clear whether this association is direct or not, but it is interesting to assume that some other protein(s) may be involved in this association. The WGA-binding proteins of molecular masses 80 and 100 kDa shown to interact with dysferlin (Fig. 4C) might be involved in this association. Alternatively, caveolin-3, reported to be dysferlin-interacting protein [25] might be involved. In the present study, we observed by biochemical analysis that caveolin-3 associated with both membranes of T-tubules and the sarcolemma (Fig. 3). This distribution pattern was consistent with previous reports [33]. We confirmed by immunoprecipitations that dysferlin in fact interacts with caveolin-3 and in addition, we found that caveolin-3 interacts with DHPR. These results show that dysferlin, DHPR and caveolin-3 may participate in the formation of a large oligomeric complex. Caveolin-3 is a major protein component of cardiac and skeletal muscle caveolae [34], another system of specialized membrane invaginations of the sarcolemma implicated in a number of cellular processes including calcium homeostasis [35] and signal transduction [36]. It has been suggested that caveolin-3 associates mainly with T-tubules during myogenesis and has been proposed to play a role in the formation of T-tubules [37]. Indeed, caveolin-3 knockout mice show a phenotype